



## DFT investigation of adsorption of pyrimidine derivatives on graphene oxide

Esvet AKBAS\*

Department of Chemistry, Faculty of Science, Van Yuzuncu Yil University, 65080 Van-Türkiye

ORCID: 0000-0001-6260-5556

Geliş Tarihi/Received	Kabul Tarihi/Accepted	Yayın Tarihi/Published
24.05.2023	09.09.2023	21.11.2023

**Abstract:** Nanomaterials have been widely used in many fields such as electronics, biomedicine, cosmetics and food processing in recent years. These materials have an important place in the development of diagnosis, treatment and prevention techniques in the field of medicine. Graphene oxide (GO), an oxidized derivative of graphene, has recently been used in biotechnology and medicine for cancer therapy, drug delivery, and cellular imaging. GO, which is widely used in many fields, can be characterized by various physicochemical properties, including its nanoscale size, surface area and electric charge. In addition, the toxic effect of GO on living cells emerges as a factor limiting its use in the medical field. In general, it has been observed that the severity of the toxic effect of this nanomaterial varies depending on the route of administration and the dose applied. In recent years, intensive studies have been initiated on the use of graphene-based materials, especially in smart medicine and gene technology. In this study, the electronic properties of commercially available pyrimidine derivative compounds and their adsorption in the graphene oxide nanocage were calculated using density functional theory (DFT).

**Keywords:** Graphene oxide, nano-biomaterial, biomedical.

### Pirimidin türevlerinin grafen oksit üzerine adsorpsiyonunun DFT araştırması

**Özet:** Nanomalzemeler son yıllarda elektronik, biyotıp, kozmetik ve gıda işleme gibi birçok alanda yaygın olarak kullanılmaktadır. Bu materyaller tıp alanında tanı, tedavi ve korunma tekniklerinin gelişmesinde önemli bir yere sahiptir. Grafenin oksitlenmiş bir türevi olan grafen oksit (GO), son zamanlarda biyoteknoloji ve tıpta kanser terapisi, ilaç dağıtımı ve hücrel görüntüleme için kullanılmaktadır. Birçok alanda yaygın olarak kullanılan GO, nano ölçekli boyutu, yüzey alanı ve elektrik yükü dahil olmak üzere çeşitli fizikokimyasal özelliklerle karakterize edilebilmektedir. Ayrıca GO'nun canlı hücreler üzerindeki toksik etkisi de tıp alanında kullanımını sınırlayan bir faktör olarak karşımıza çıkmaktadır. Genel olarak bu nanomateryalin toksik etkisinin şiddetinin uygulama yoluna ve uygulanan doza bağlı olarak değiştiği gözlemlenmiştir. Son yıllarda grafen bazlı materyallerin özellikle akıllı tıp ve gen teknolojisinde kullanımına yönelik yoğun çalışmalar başlatıldı. Bu çalışmada, ticari olarak temin edilebilen pirimidin türevi bileşiklerin elektronik özellikleri ve bunların grafen oksit nanokafesindeki adsorpsiyonları, yoğunluk fonksiyonel teorisi (DFT) kullanılarak hesaplanmıştır.

**Anahtar Kelimeler:** Grafen oksit, nano-biyometeryal, biyomedikal.

## 1. INTRODUCTION

Graphene oxide obtained by the oxidation of graphene is a remarkable material due to the oxygen, hydroxy and carboxylic acid groups it contains on its surface [1] (Fig. 1).

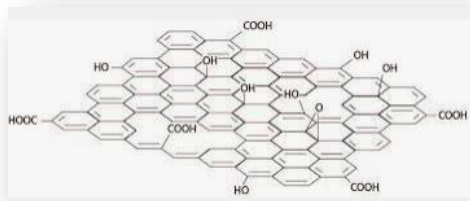


**Figure 1.** Surface of graphene oxide.

Graphene oxide shows a layered structure due to the epoxy and hydroxyl groups it contains on its surface [2-6]. In graphene oxide, the carbon atoms found  $sp^2$  hybridization. The p orbital outside the plane provides the electron delocalization network [7]. Because of this feature, graphene oxide has good optical, thermal, magnetic and electrical properties. This situation expands the usage areas of graphene oxide in materials engineering [8, 9]. The biocompatibility and very large surface area of graphene oxide also facilitates its use in drug/gene delivery and tissue engineering fields [10].

The interaction of aromatic heterocyclic compounds with surfaces is of practical importance for a wide range of applications, from heterogeneous catalysis to corrosion protection [11]. For example, breaking the C-S bond on the adsorption surfaces of thiophene is an important step in elucidating the hydrodesulfurization mechanism [12]. Adsorption of furan to relevant surfaces is also of great importance in the catalytic transformation of value-added furan compounds [13]. Most importantly, the adsorption of aromatic heterocyclic molecules to surfaces plays a vital role in their transport mechanism [14]. To form a carrier film, aromatic heterocyclic compounds must be adsorbed onto the surface of the molecule. Heteroatoms (N, O, S) in aromatic heterocyclic compounds participate in the conjugated  $\pi$  bond system in the aromatic ring and play a role in enhancing the adsorption of molecules.

Density functional theory (DFT) has proven to be a useful method in studying the adsorption of organic compounds and investigating its mechanism [15]. Parameters such as adsorption energy of molecule-carrier surface interaction, electronic interaction and charge transfer between molecule-surface can be obtained from the results of DFT calculations [16]. In a related DFT study, Lei Guo and co-workers [16] calculated the adsorption energies of pyrrole, furan, and thiophene on the surface to verify the empirical rule for

the adsorption efficiency of organic compounds. However, the surface binding mechanism of adsorbates has not been sufficiently characterized in their studies.

Organic molecules containing heteroatoms are key molecules in drug design. Many anticancer drugs with these groups are widely used today. Heteroatomic compounds, which are of pharmaceutical importance and widely used, are compounds containing nitrogen, oxygen and sulfur.

Among the heterocyclic structures containing more than one nitrogen, pyrimidine derivatives are the most interesting group [17], and one reason for this is that pyrimidine compounds are also found in folic acid, caffeine and vitamin B2, DNA and RNA. It has also been reported that pyrimidine-derived compounds are very important for the design and synthesis of potent anticancer drugs. In recent years, many pyrimidine compounds with chemotherapeutic properties have been synthesized and used clinically.

It is also known that pyrimidine derivatives have many biological activities. These compounds are of vital importance in this field because they can be synthesized commercially, their chemistry can be elucidated, and they are used as structural components in the pharmaceutical industry. Recently, unnatural nucleoside analogues with pyrimidine ring system have been widely used in the development of new generation anticancer drugs [20].

In this study, we perform a systematic study on the adsorption of the 5-(4-formylphenyl) pyrimidine (**1**) (Sigma-Aldrich, 647136), pyrimidine-2-carboxylic acid (**2**) (Merck, 754315), pyrimidine-5-carboxylic acid (**3**) (Merck, 718769), methyl pyrimidine-5-carboxylate (**4**) (Merck, 754315), 2-(ethylthio)pyrimidine-5-carbaldehyde (**5**) (Merck, CBR00455) (Fig. 2) on the graphene oxide surface through DFT calculations, focusing on understanding the surface binding mechanism of adsorbates.

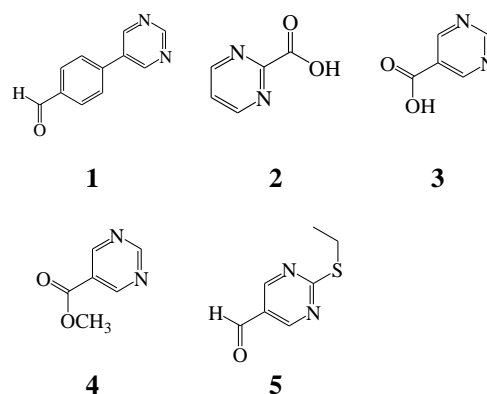


**Figure 2.** Molecular structures of studied compounds

## 2. MATERIALS AND METHOD

## 2.1. Computational methods

The adsorption of pyrimidine derivative compounds on the surface of the graphene oxide was investigated by density functional theory calculations. The calculations are made on Gaussian09 program using the BPV86 functional with the basis set 6-31 G' (d, p) [21]. This basis set is very useful for nanostructural frameworks [22, 23]. To accurately predict the weak interaction, the adsorption energies ( $\Delta E_{ad}$ ) were calculated as follows:

$$\Delta E_{ad} = E(\text{complex}) - \Delta E(\text{graphene oxide}) - \Delta E(\text{substrate}) \quad (1)$$

Quantum chemical parameters  $\Delta E_{HOMO}$ ,  $\Delta E_{LUMO}$  and energy gap ( $\Delta E$ ) were calculated and discussed for all types of interactions. In addition, ionization potential "I", electron affinity "A", chemical softness "S", dipole moment " $\mu$ ", chemical hardness " $\eta$ " and electronegativity " $\chi$ " [24,25] calculations have been carried out for graphene oxide and substrates.

## 3. RESULTS AND DISCUSSION

Full geometry optimizations of the graphene oxide, substrates and all interactions were performed using density functional theory based on BPV86 and the 6-31 G' (d, p) basis set in Gaussian09 program [21,26] (Fig. 3).

Looking at the calculations for graphene oxide, it is seen that the electron density is concentrated on the epoxy group, while the electrophilic density is concentrated on the carboxylic acid group.

The highest energy occupied orbital and lowest energy vacant orbital values of the molecules obtained by theoretical calculations are very important parameters in estimating the adsorption activities of molecules. In order to determine the adsorption characteristics of molecules, besides these parameters, the gap energy value, ionization potential, electron affinity, chemical softness and chemical hardness values, electronegativity values and dipole moments of the molecules must be calculated.

According to Koopman's [27],  $E_{HOMO}$  and  $E_{LUMO}$  of the molecule are related to the ionization potential (I) and the electron affinity (A), respectively. And the electronegativity ( $\chi$ ) and chemical hardness ( $\eta$ ) can be calculated as follows: [28]. Like chemical hardness ( $\eta$ ), chemical softness (S) is a global chemical descriptor that measuring molecular stability and can be calculated as follows: [28]. The data obtained as a result of the calculations are given in the table 1.

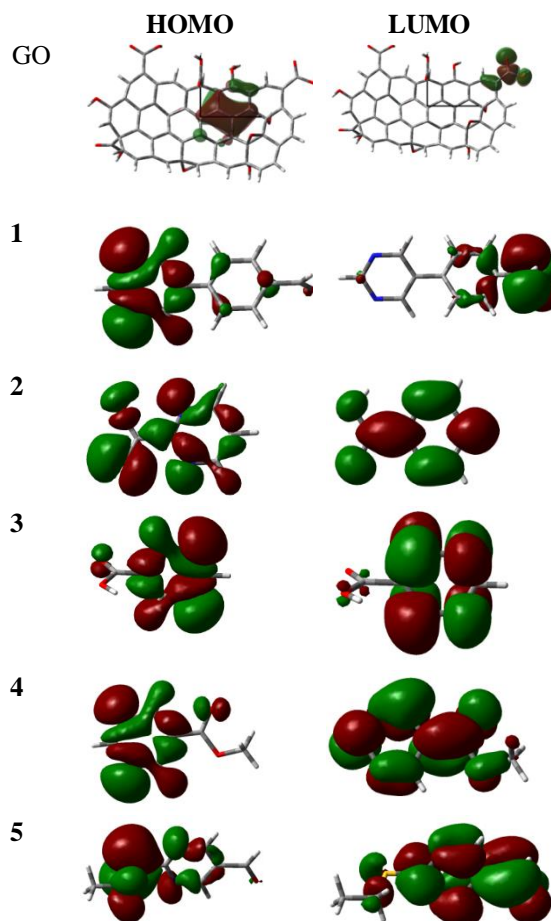


**Figure 3.** Optimized structures and HOMO and LUMO profile

$$\chi = -\mu = \left( \frac{-E_{HOMO} - E_{LUMO}}{2} \right) = \left( \frac{I + A}{2} \right) \quad (2)$$

$$\eta = \frac{1}{2} \left( \frac{\partial^2 E}{\partial N^2} \right)_{\theta(r)} = \frac{1}{2} \left( \frac{\partial \mu}{\partial N} \right) \quad (3)$$

$$S = \frac{1}{\eta} \quad (4)$$

**Table 1.** The quantum chemical parameters (eV).

	$E_{HOMO}$	$E_{LUMO}$	$\Delta E$	I	A
GO	-7.169	-0.975	6.194	7.169	0.975
1	-5.385	-2.255	3.129	5.385	2.255
2	-6.024	-3.144	2.880	6.024	3.144
3	-6.250	-2.658	3.591	6.250	2.658
4	-5.621	-3.042	2.579	5.621	3.042
5	-5.265	-3.510	1.755	5.265	3.510
	$\eta$	S	$\chi$	$\mu$ (D)	
GO	6.1943	0.1614	4.0722	6.4721	
1	3.1297	0.3195	3.8203	1.9989	
2	2.8805	0.3472	4.5846	6.3818	
3	3.5919	0.2784	4.4545	2.8341	
4	2.5796	0.3877	4.3320	1.7996	
5	1.7551	0.0001	4.3877	2.4877	

### 3.1. Non-linear optical (NLO) properties

The nonlinear optical properties of all compounds were obtained in the gas phase. The total dipole moment  $\mu_{tot}$ , mean polarizability ( $\alpha_{tot}$ ) and mean first hyperpolarizability ( $\beta_{tot}$ ) can be calculated using the following equations.

$$\mu_{tot} = \mu_x^2 + \mu_y^2 + \mu_z^2 \quad (5)$$

$$\alpha_{tot} = (\alpha_{xx} + \alpha_{yy} + \alpha_{zz})/3 \quad (6)$$

$$\beta_{tot} = [(\beta_{xxx} + \beta_{xyy} + \beta_{xzz})^2 + (\beta_{yxx} + \beta_{yxx} + \beta_{yzz})^2 + (\beta_{zzz} + \beta_{zxx} + \beta_{zyy})^2]^{1/2} \quad (7)$$

The obtained values are given in Table 2. Based on these results, it can be said that the compounds with the highest hyperpolarizability have more active NLO properties.

Molecular electrostatic potential maps (MEPs) of all compounds and graphene substrate interactions were calculated (Figure 4). The electrostatic potential increases during red > orange > yellow > green > blue. The negative (red) are associated with electrophilic reactivity and positive (blue) areas with nucleophilic reactivity. The highest potential is on oxygen atoms.

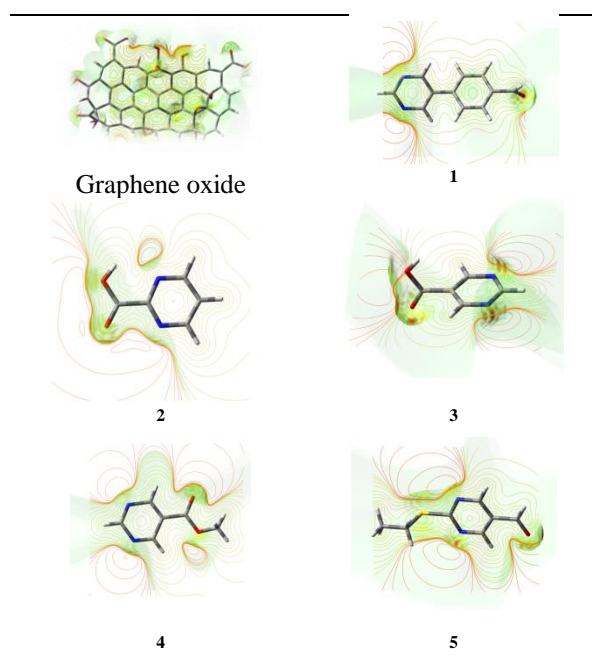


**Figure 4.** Molecular electrostatic potential maps (MEPs) for all compounds

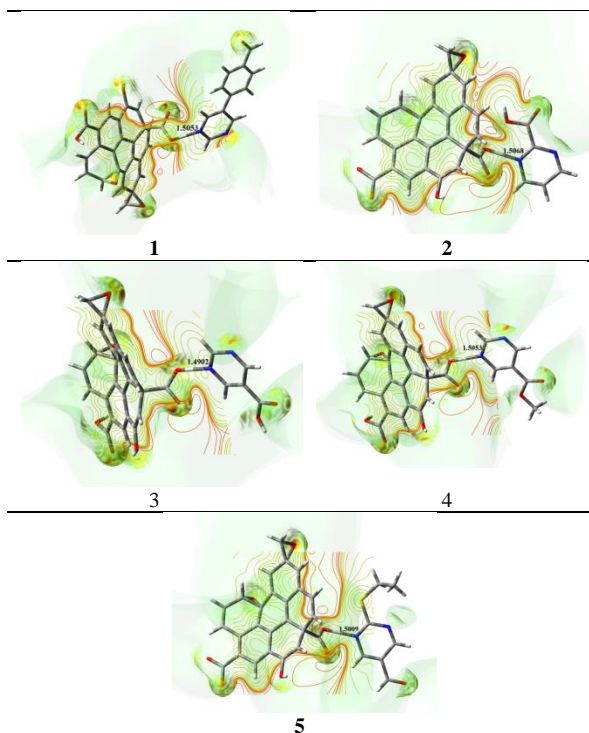
**Table 2.** Electric dipole moment  $\mu$ , polarizability  $\alpha$  and first hyperpolarizability  $\beta$  values

Parameters (a.u)	GO	1	2
$\beta_{xxx}$	589.89	-51.2861	43.2751
$\beta_{xyy}$	155.75	30.9538	6.3079
$\beta_{xzz}$	-60.71	5.2783	-8.5466
$\beta_{yyy}$	-269.39	0.1079	14.1085
$\beta_{yxx}$	-228.15	30.9538	7.1573
$\beta_{yzz}$	78.01	0.0559	-0.3934
$\beta_{zzz}$	-51.68	-1.9739	0.0003
$\beta_{xxz}$	69.49	40.1973	-0.0006
$\beta_{zyy}$	7.41	0.1031	0.0005
$\beta_{tot}$ (esu) $10^{-33}$	803.6	175.48	46.0396
$\alpha_{xx}$	17.96	-94.0551	-49.3057
$\alpha_{yy}$	-1.52	-75.9239	-49.5436
$\alpha_{zz}$	-16.43	-81.1604	-49.9552
$\alpha_{tot}$ (esu) $10^{-33}$	-0.01	-284.624	-168.645
$\mu_x$	4.30	0.6648	5.8184
$\mu_y$	-4.67	0.6451	2.6216
$\mu_z$	1.23	1.7713	0.0000
$\mu_{tot}$ (esu) $10^{-33}$	22.00	23.10	21.69

Parameters (a.u)	GO	4	5
$\beta_{xxx}$	589.89	29.20	-76.78
$\beta_{xyy}$	155.75	13.36	14.13
$\beta_{xzz}$	-60.71	6.63	3.60
$\beta_{yyy}$	-269.39	1.66	-1.58
$\beta_{yxx}$	-228.15	-14.77	32.24
$\beta_{yzz}$	78.01	0.86	-0.54
$\beta_{zzz}$	-51.68	-0.31	3.53
$\beta_{xxz}$	69.49	6.46	10.88
$\beta_{zyy}$	7.41	-0.29	4.60
$\beta_{tot}$ (esu) $10^{-33}$	803.6	51.04	68.95
$\alpha_{xx}$	17.96	-50.88	-70.27
$\alpha_{yy}$	-1.52	-61.58	-71.89
$\alpha_{zz}$	-16.43	-56.16	-70.22
$\alpha_{tot}$ (esu) $10^{-33}$	-0.01	-56.20	-70.79
$\mu_x$	4.30	1.22	-0.33
$\mu_y$	-4.67	-1.14	1.55
$\mu_z$	1.23	0.66	1.91
$\mu_{tot}$ (esu) $10^{-33}$	22.00	6.11	8.45

The interaction of each compound with graphene oxide, the bond length ( $\text{\AA}$ ) and electronic maps resulting from the interaction are as given in Figure 5.



**Figure 5.** All interaction of complexes

The bonding geometries and bond lengths of all complexes were calculated. Consequently, complex **3** is the most stable due to the interaction between compounds and the graphene oxide nanocage from its N group side ( $1.4902\text{\AA}$ <sup>0</sup>).

Calculation of the energies of the complexes showed that the electronic and adsorption energy for complex **2** was approximately  $\Delta E_{(\text{complex})} -52798.59$  (eV) and  $\Delta E_{\text{ad}} 1.64$  (eV) (Table 3).

**Table 3.** Calculated were electronic energies for complexes.

Complexes	$\Delta E_{(\text{complex})}$ (eV)	$\Delta E_{\text{ad}}$ (eV)
<b>1</b>	-40475.81	0.35
<b>2</b>	-52798.59	1.64
<b>3</b>	-52799.68	0.28
<b>4</b>	-53868.80	-0.27
<b>5</b>	-63727.62	0.002

When the adsorption energies are compared, it is seen that **2** has a higher adsorption energy value. Accordingly, the two main mechanisms involved in the adsorption of compounds to the carboxylic acid site on the graphene oxide nanocage surface are orbital and charge-induced interactions (electrostatic effect). In particular, the hydrogen atom bonded to the nitrogen atom interacts with the oxygen in the carboxylic acid group, inducing intermolecular electrostatic interactions. Consequently, complex **2** is the most stable from its N side due to the interaction between compound and the graphene oxide nanocage.

### 3.2. Density of states analysis

Figure 6 shows the density of the state spectra for compound **2** and complex **2**. The decrease in the  $E_g$  value of the graphene oxide-substrate compared to the graphene oxide nanocage is due to this opposite Electric Peak after the adsorption process of substrate. Furthermore, a closer examination of the DOS spectrum reveals that the HOMO and especially the LUMO levels are shifted to the higher energy region after adsorption of substrate.

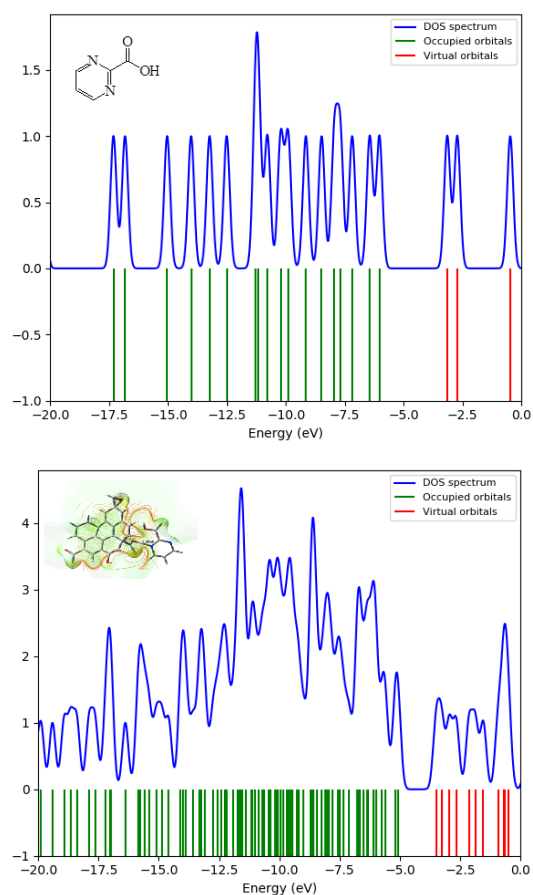


**Figure 6.** DOS plots of pristine compound **2** and complex **2**

## 4. CONCLUSIONS

The interaction between substrate and the graphene oxide nanocage were evaluated using DFT calculations to find a novel substrate sensing system. Studies show that the adsorption occurs as a result of the interaction of the COOH groups on the graphene oxide nanolattice surface and the N atoms in the substrate. The adsorption mechanism is also accompanied by electrostatic interactions.

When the bond lengths are compared, it is seen that there is no big difference between compound **2** and

compound **3**, but compound **2** is higher in terms of adsorption energy. In this case, compound **2** is the most stable by N due to the interaction between the compounds and the graphene oxide nanocage

**Conflicts of Interest:** The authors declare no competing financial interest.

**Ethical Approval:** Ethics Approval is not required for this study.

## REFERENCES

- [1] K. Krishnamoorthy, G.S. Kim, S.J. Kim, "Graphene Nanosheets: Ultrasound Assisted Synthesis and Characterization", *Ultrason, Sonochem.* (2013), 20 644–649.
- [2] F. Mouhat, F. X. Coudert, L. M. Bocquet, "Structure and chemistry of graphene oxide in liquid water from first principles", *Nature Communications*, (2020), 11(1)1566.
- [3] L. Valentini, S. Bittolo Bon, G. Giorgi, "Engineering graphene oxide/water interface from first principles to experiments for electrostatic protective composites", *Polymers (Basel)*, (2020), 12(7) 1596.
- [4] G.K. Ramesha, A.V. Kumara, H.B. Muralidhara, S. Sampath, "Graphene and graphene oxide as effective adsorbents toward anionic and cationic dyes", *Journal of Colloid Interface science*, (2011), 361 270–277.
- [5] J. Zhu, S. Wei, H. Gu, S.B. Rapole, Q. Wang, Z. Luo, N. Haldolaarachchige, D.P. Young, Z. Guo, "One-Pot Synthesis of Magnetic Graphene Nanocomposites Decorated with Core@Double-shell Nanoparticles for Fast Chromium Removal", *Environmental science & technology*, (2012), 46 (2) 977–985.
- [6] J.N. Tiwari, K. Mahesh, N.H. Le, K.C.K.R. Timilsina, R.N. Tiwari, K.S. Kim, "Reduced graphene oxide-based hydrogels for the efficient capture of dye pollutants from aqueous solutions", *Carbon*, (2013), 56 173–182.
- [7] J. Bai, X. Zhong, S. Jiang, Y. Huang, X. Duan, "Graphene nanomesh", *Nature material*, (2010), 5 190–194.
- [8] Z. Li, J. Fan, C. Tong, et al., "A smart drug-delivery nanosystem based on carboxylated graphene quantum dots for tumor-targeted chemotherapy", *Nanomedicine*, (2019), 14(15) 2011–2025.
- [9] Fedotova, A. K., Prischepa, S. L., Fedotova, J., et al., "Electrical conductivity and magnetoresistance in twisted graphene electrochemically decorated with Co particles", *Physica E: Low-dimensional Systems and Nanostructures*, (2020), 117 113790.
- [10] J.H. Jiang, et al., "Functional graphene oxide as cancer-targeted drug delivery system to selectively induce oesophageal cancer cell apoptosis", *Arti Cells Nanomed Biotechnol*, (2018), 46(3) 297–S307.
- [11] S.J. Jenkins, "Aromatic adsorption on metals via first-principles density functional theory", *Proceedings of the Royal Society A: Mathematical, Physical and Engineering Sciences*, (2009), 465, 2949–2976.
- [12] H. W. Zhu, M. Guo, L. Li, S. Zhao, et al., "Density Functional Theory Study of the Adsorption and Desulfurization of Thiophene and Its Hydrogenated Derivatives on Pt(111): Implication for the Mechanism of Hydrodesulfurization over Noble", *Metal Catalysts, ACS Catalysis*, (2011), 1, 1498–1510.
- [13] S. Wang, V. Vorotnikov, D.G. Vlachos, "A DFT study of furan hydrogenation and ring opening on Pd(111)", *Green Chemistry*, (2014), 16, 736–747.
- [14] M. Goyal, S. Kumar, I. Bahadur, C. Verma, E.E. Ebenso, "Organic corrosion inhibitors for industrial cleaning of ferrous and non-ferrous metals in acidic solutions: A review", *Journal of Molecular Liquids*, (2018), 256, 565–573.
- [15] E. Ebenso, C. Verma, L. Olasunkanmi, E.D. Akpan, D. Verma, H. Lgaz, L. Guo, S. Kaya, M.A. Quraishi, "Molecular modeling of compounds used for corrosion inhibition studies: A review", *Physical Chemistry Chemical Physics journal*, (2021).
- [16] L. Guo, I.B. Obot, X. Zheng, X. Shen, Y. Qiang, S. Kaya, C. Kaya, "Theoretical insight into an empirical rule about organic corrosion inhibitors containing nitrogen, oxygen, and sulfur atoms", *Applied Surface Science*, (2017), 406, 301–306.
- [17] M. Schnürch, M. D. Mihovilovic, "Topics in Heterocyclic Chemistry, in: P. C. Gros (Eds), *Metalation of Azines and Diazines*", Springer-Verlag Berlin Heidelberg, New York, Dordrecht, London, (2013), 1, 20.
- [18] S.A. Rahaman, Y. Rajendra Pasad, P. Kumar, B. Kumar, "Synthesis and anti-histaminic activity of some novel pyrimidines", *Saudi Pharm Journal*, (2009), 17, 255.
- [19] E. Akbas, K.A. Othman, F.Ç. Çelikezen, N. A. Ejder, H. Turkez, O. E. Yapca, A. Mardinoglu, "Synthesis and Biological Evaluation of Novel Benzylidene Thiazolo Pyrimidin-3(5H)-One Derivatives" *Polycyclic Aromatic Compounds*,

- (2022), <https://doi.org/10.1080/10406638.2023.228961>
- [20] A. D. Becke, "Density-functional thermochemistry. III. The role of exact exchange" *Journal of Chemical Physics*, (1993), 98, 1372.
- [21] Gaussian 09, Revision D.01, M. J. Frisch, G. W. Trucks, et al., Gaussian, Incremental, Wallingford, CT, USA, (2009).
- [22] J. P. Perdew, Y. Wang, "Accurate and Simple Analytic Representation of the Electron-Gas Correlation Energy", *Physical Review B - Condensed Matter and Materials*, (1992), 45, 13244–13249.
- [23] T. E. Simos, C. Tsitouras, V. N. Kovalnogov, R. V. Fedorov, D. A. Generalov, "Real-Time Estimation of R0 for COVID-19 Spread", *Mathematics (Basel)*, (2021), 9, 664.
- [24] Y. Karzazi, M.E. A. Belghiti, A. Dafali, and B. Hammouti, "A theoretical investigation on the corrosion inhibition of mild steel by piperidine derivatives in hydrochloric acid solution", *Journal of Chemical and Pharmaceutical Research*, (2014), 6(4) 689-696.
- [25] E. D. Glendening, C. R. Landis, F. Weinhold, "NBO 6.0: Natural Bond Orbital Analysis", Program. *Journal of Computational Chemistry*, (2013), 341429–1437.
- [26] C. Lee, W. Yang, R. G. Parr, "Development of the Colle-Salvetti correlation-energy formula into a functional of the electron density", *Physical Review B*, (1988), 37, 785.
- [27] H. Wang, X. Wang, H. Wang, L. Wang, A. Liu, "DFT study of new bipyrazole derivatives and their potential activity as corrosion inhibitors", *Journal of Molecular Modeling*, (2007), 13, 147.
- [28] I. Fleming, *Frontier Orbitals and Organic Chemical Reactions*, John Wiley and Sons, NewYork. (1976).